

Multi-Label Annotation Aggregation in Crowdsourcing

Xuan Wei*

Daniel Dajun Zeng[†]

Junming Yin[‡]

June 19, 2017

Abstract

As a means of human-based computation, crowdsourcing has been widely used to annotate large-scale unlabeled datasets. One of the obvious challenges is how to aggregate these possibly noisy labels provided by a set of heterogeneous annotators. Another challenge stems from the difficulty in evaluating the annotator reliability without even knowing the ground truth, which can be used to build incentive mechanisms in crowdsourcing platforms. When each instance is associated with many possible labels *simultaneously*, the problem becomes even harder because of its combinatorial nature. In this paper, we present new flexible Bayesian models and efficient inference algorithms for multi-label annotation aggregation by taking both annotator reliability and label dependency into account. Extensive experiments on real-world datasets confirm that the proposed methods outperform other competitive alternatives, and the model can recover the type of the annotators with high accuracy. Besides, we empirically find that the mixture of multiple independent Bernoulli distribution is able to accurately capture label dependency in this unsupervised multi-label annotation aggregation scenario.

1 Introduction

Crowdsourcing has emerged as a cost-effective tool to harness the power of human computation to annotate large-scale unlabeled datasets. These tasks, such as image tagging and video annotation, are often too repetitive and time-consuming for individuals to complete [11]. Many crowdsourcing systems, such as Amazon Mechanical Turk (AMT), provide a platform where a large amount of tasks can be distributed to human workers and then the results are aggregated together. Such systems have recently started to play a vital role in industry. For example, Google launched Image Labeler [1] to allow users to annotate random images so as to improve the performance of the image search engine. reCAPTCHA has been adopted by many websites where users are asked to solve captchas to prove they are humans, then the captchas are utilized to digitize scanned articles and books [8].

Academic communities are also increasingly attracted to use crowdsourcing for their research needs. For instance, to create taxonomy for large amount of entities, [3] recruits workers from AMT to label the relationship between entities; [18] relies on AMT to construct a training set for coding the sentiments of online comments, where the results are further utilized to construct reputation measure.

Although promising, crowdsourcing for annotation aggregation still faces many significant challenges. In practice, annotators may come from a diverse pool including experts, novices, spammers,

*Eller College of Management, University of Arizona, Tucson, AZ 85721. Email: weix@email.arizona.edu

[†]Eller College of Management, University of Arizona, Tucson, AZ 85721. Email: zeng@email.arizona.edu

[‡]Eller College of Management, University of Arizona, Tucson, AZ 85721. Email: junmingy@email.arizona.edu

and even malicious annotators [21]. Moreover, unintentional errors are common because most crowdsourcing tasks are tedious [14]. Hence, a fundamental challenge in crowdsourcing applications is how to accurately and efficiently estimate the ground truth from these noisy labels provided by a set of heterogeneous annotators. Another challenge comes from the evaluation of annotation reliability since the ground truth is often unknown in practice. Annotator evaluation can not only improve the aggregation performance [12], but can also serve as a spammer detector [21] and help design better incentive mechanisms (e.g., performance-based payments [10]).

In the previous literature, the problem of *multi-class* annotation aggregation has been intensively studied to address the aforementioned challenges [19, 15, 21, 30, 28, 7, 22]. However, there is very little work focusing on *multi-label* annotation aggregation. In certain application areas, it's quite common that each instance is associated with a subset of label candidates simultaneously (see [24, 29] and references therein). For instance, a document may contain multiple topics or ideas, and an image can be assigned with multiple tags. Due to combinatorial explosion in the number of possible label combinations, multi-label annotation aggregation is particularly more difficult. One simple heuristic is to treat each label independently and transform the problem into multiple binary tasks. Such heuristic completely ignores the label dependency that is likely to arise in real-world applications (though unknown in the label collection step of crowdsourcing pipeline) and the resulting procedure might lead to sub-optimal or even incorrect estimation. Therefore, it is crucial to take such dependency into account so as to improve the overall performance of multi-label aggregation. For example, a document labeled with **military** is more likely to be associated with **politics** rather than **education** or **health**, and quiet music is often lonely music as well as being relaxing music.

At the other extreme, we can model dependency among C labels by explicitly using 2^C parameters to represent $P = \{p_S | S \subseteq \{1, 2, \dots, C\}\}$, where p_S is the probability of an instance's labels being equal to S . Some existing approaches include the power set approach [24], the additive model [5], and the multivariate Bernoulli distribution [6]. Though all orders of interactions can be characterized, these approaches are limited in that (1) they are computationally demanding and hence are only applicable when C is fairly small and (2) the estimation of 2^C parameters could be highly biased unless the sample size is fairly large. Other intermediate methods between these two extremes, such as Ising model [26], only consider second-order relations to model P with $\mathcal{O}(C^2)$ parameters. However, capturing only pairwise dependency is insufficient especially in certain real-world applications where there exist many higher-order interactions.

In this paper, we propose to use the mixture of multiple Bernoulli distribution [16, 2], with the hope that only a fairly small number of mixture components need to be combined to capture intrinsic label dependency. Mixture of multiple Bernoulli distribution has been utilized to model label dependency for *supervised* multi-label classification task; see [17] and references therein. However, to the best of our knowledge, there is no work on demonstrating its role in the context of *unsupervised* multi-label annotation aggregation, in which only noisy labels are available.

Overall, we make the following contributions in this work: (a) Building on top of the mixture of multiple Bernoulli distribution, we develop a flexible Bayesian model for observed annotations by taking both annotator reliability and label dependency into account; (b) We propose an efficient inference algorithm to perform annotation aggregation from possibly noisy labels in an unsupervised manner; (c) Results on three real-world datasets confirm that our new approaches outperform other competitive alternatives in terms of recovering ground truth labels. The methods are also able to capture the observed label dependency and recover the type of annotators with high accuracy.

τ_j of $\boldsymbol{\tau} \in [0, 1]^C$ specifies the probability of an instance having the label j . Conditioning on $\boldsymbol{\tau}$, the ground truth $z_{i,j}$ follows

$$z_{i,j} \mid \tau_j \sim \text{Bernoulli}(\tau_j). \quad (1)$$

Given the ground truth \mathbf{z} and annotator reliability $\boldsymbol{\Psi}$, we have the following model for observed annotations \mathbf{Y} :

$$y_{i,j}^l \mid \boldsymbol{\Psi}, \mathbf{z} \sim \text{Bernoulli}(\Psi_j^l z_{i,j} + (1 - \Psi_j^l)(1 - z_{i,j})). \quad (2)$$

We also introduce priors over the parameters Ψ_j^l and τ_j . In particular, we use conjugate prior distributions

$$\begin{aligned} \Psi_j^l \mid a, b &\sim \text{Beta}(a, b), \\ \tau_j \mid \alpha, \beta &\sim \text{Beta}(\alpha, \beta). \end{aligned} \quad (3)$$

Here, the hyperparameters a, b indicate how strong our prior belief is about the reliability of annotators, while α, β specify our prior belief about the number of present labels. The choice of those hyperparameters is often context-dependent. See experimental section for more details.

2.3 BMMB Model

In the BNC model, the label correlations are ignored and hence the problem reduces to C independent binary annotation aggregation tasks (one per label). However, as we have already pointed out, label dependency is likely to arise in practice and it is important to be incorporated to improve the performance of multi-label related tasks (multi-label aggregation [9] and multi-label learning [29]). We propose to use the mixture of multiple independent Bernoulli distribution, which offers a flexible and powerful framework for modeling label dependency.

Specifically, in our Bayesian model with Mixture of Multiple Bernoulli distribution (BMMB), we assume that there are K clusters with each cluster k being a multiple independent Bernoulli distribution, which is parameterized by $\boldsymbol{\tau}_k \in [0, 1]^C$. The mixing coefficient π_k indicates the probability of an instance belonging to the cluster k . Under this setup, in contrast to the independent assumption in the BNC model (1), the ground truth $\mathbf{z}_i \in \{0, 1\}^C$ has the following probability distribution:

$$p(\mathbf{z}_i \mid \boldsymbol{\pi}, \boldsymbol{\tau}_k) = \sum_{k=1}^K \pi_k \prod_{j: z_{i,j}=1} \tau_{k,j} \prod_{j: z_{i,j}=0} (1 - \tau_{k,j}). \quad (4)$$

The graphical model representation of the BMMB model is shown in Figure 1b, where we introduce a latent variable $x_i \in \{1, 2, \dots, K\}$ to represent the cluster index of the instance i . In summary, we have the following observational model:

$$\begin{aligned} y_{i,j}^l \mid \boldsymbol{\Psi}, \mathbf{z} &\sim \text{Bernoulli}(\Psi_j^l z_{i,j} + (1 - \Psi_j^l)(1 - z_{i,j})), \\ z_{i,j} \mid x_i, \boldsymbol{\tau} &\sim \text{Bernoulli}(\tau_{x_i,j}), \\ x_i \mid \boldsymbol{\pi} &\sim \text{Discrete}(\boldsymbol{\pi}). \end{aligned} \quad (5)$$

Similarly, we impose conjugate priors over the parameters Ψ_j^l , $\tau_{k,j}$, and $\boldsymbol{\pi}$ as follows:

$$\begin{aligned} \Psi_j^l \mid a, b &\sim \text{Beta}(a, b), \\ \tau_{k,j} \mid \alpha, \beta &\sim \text{Beta}(\alpha, \beta), \\ \boldsymbol{\pi} \mid \gamma &\sim \text{Dirichlet}(\boldsymbol{\gamma}). \end{aligned} \quad (6)$$

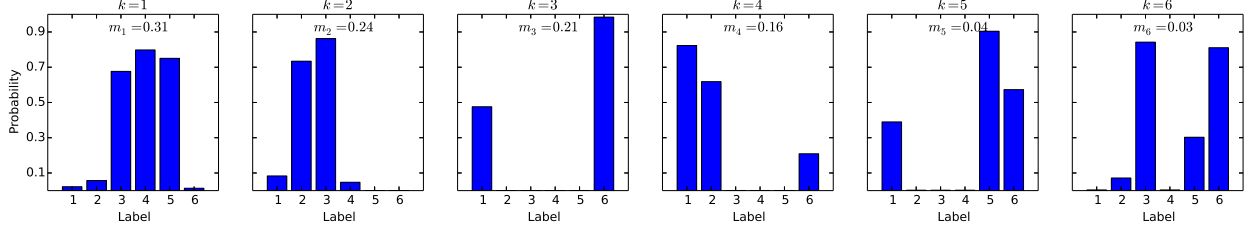


Figure 2: Estimated 6 mixture components by the BMMB model from the Emotions dataset; see Section 4 for details. Each bar represents the probability of the corresponding label within that mixture component (i.e., $\tau_{k,j}$). m_k is the estimated mixing proportion of the k -th component. The 6 labels in x-axis, from left to right, are "amazed-surprised", "happy-pleased", "relaxing-calm", "quiet-still", "sad-lonely", and "angry-aggressive", respectively.

An illustrative example. We use an illustrative example to demonstrate how exploiting label dependency in the BMMB model can improve the performance. The Emotions [23] dataset consists of hundreds of music pieces with 6 pre-defined labels. We generate random noisy annotations that are provided by annotators with varying reliability (see Section 4 for details). For one particular music piece with true labels $\{3, 4, 5\}$ ("relaxing-calm", "quiet-still", "sad-lonely"), the probabilities of having these labels estimated by the BNC model are 1.0000, 0.0643, and 0.9998, respectively. As a consequence, the label "quiet-still" is missed by the BNC estimate. In contrast, the corresponding probabilities estimated by the BMMB model with $K = 6$ components are 1.000, 0.996, and 1.000, respectively, which shows the effectiveness of modeling label dependency. We can gain more insight by examining the estimated mixture components. As shown in Figure 2, the major components all characterize certain type of label dependency. For instance, (1) the first component indicates that quiet music tends to be relaxing, calm, and lonely; (2) intuitively, happy and pleased music is quite likely to be relaxing and calm (the second component); (3) when one piece of music is emotional, it may have labels "amazed-surprised" and "angry-aggressive" together (the third component). Interestingly, the BMMB estimate concludes that the selected sample is extremely likely from the first mixture component (with probability being almost 1.0), which is the one that mainly captures the dependency among the true labels $\{3, 4, 5\}$.

3 Inference Algorithm

In this section, we develop a mean-field variational inference algorithm [13, 26] for performing approximate inference under our BMMB model². The true posterior of latent variables $p(\Psi, \mathbf{z}, \boldsymbol{\tau}, \mathbf{x}, \boldsymbol{\pi} \mid \mathbf{Y}, a, b, \alpha, \beta, \gamma)$ is approximated by a fully factorized variational distribution $q(\Psi, \mathbf{z}, \boldsymbol{\tau}, \mathbf{x}, \boldsymbol{\pi})$ where

$$q(\Psi, \mathbf{z}, \boldsymbol{\tau}, \mathbf{x}, \boldsymbol{\pi}) = q(\Psi \mid \mathbf{g}, \mathbf{h})q(\mathbf{z} \mid \boldsymbol{\lambda})q(\boldsymbol{\tau} \mid \mathbf{e}, \mathbf{f})q(\mathbf{x} \mid \mathbf{r})q(\boldsymbol{\pi} \mid \mathbf{m}). \quad (7)$$

Specifically, the posteriors Ψ_j^l and $\tau_{k,j}$ follow the distributions $\text{Beta}(g_j^l, h_j^l)$ and $\text{Beta}(e_{k,j}, f_{k,j})$, respectively; the posterior $q(z_{i,j})$ is parameterized as $q(z_{i,j}) = \text{Bernoulli}(\lambda_{i,j})$; the posterior $q(x_i)$ is parameterized as $q(x_i) = \text{Discrete}(\mathbf{r}_i)$; and the posterior $q(\boldsymbol{\pi})$ follows the $\text{Dirichlet}(\mathbf{m})$. For ease of presentation, we denote all variational parameters as $\theta_v = \{\mathbf{g}, \mathbf{h}, \boldsymbol{\lambda}, \mathbf{e}, \mathbf{f}, \mathbf{r}, \mathbf{m}\}$ and all hyperparameters as $\theta_h = \{a, b, \alpha, \beta, \gamma\}$.

²The inference procedure for the BNC model is similar. See Appendix B for more details.

The variational inference aims to minimize the KL divergence $\text{KL}(q\|p)$ between the approximating distribution q and the true but unknown posterior p . It is well-known that the log marginal likelihood $\log(\mathbf{Y} \mid \theta_h)$ can be decomposed in the form of $\log(\mathbf{Y} \mid \theta_h) = \mathcal{L}(\theta_v) + \text{KL}(q\|p)$, where

$$\mathcal{L}(\theta_v) = \mathbb{E}_q[\log p(\mathbf{Y}, \boldsymbol{\Psi}, \mathbf{z}, \boldsymbol{\tau}, \mathbf{x}, \boldsymbol{\pi} \mid \theta_h)] - \mathbb{E}_q[\log q(\boldsymbol{\Psi}, \mathbf{z}, \boldsymbol{\tau}, \mathbf{x}, \boldsymbol{\pi})] \quad (8)$$

is known as the Evidence Lower Bound (ELBO). Therefor, minimizing the KL divergence is equivalent to maximizing the ELBO with respect to the variational parameters θ_v . The exact form of the ELBO $\mathcal{L}(\theta_v)$ for the BMMB model is provided in Appendix A. Applying coordinate ascent algorithm iteratively to maximize $\mathcal{L}(\theta_v)$, we obtain the following update rules.

- Updates for \mathbf{g}, \mathbf{h} : for $j = 1, \dots, C$ and $l = 1, \dots, L$,

$$g_j^l = a + \sum_{i \in N(l)} \{\lambda_{i,j} y_{i,j}^l + (1 - \lambda_{i,j})(1 - y_{i,j}^l)\}, \quad h_j^l = b + \sum_{i \in N(l)} \{\lambda_{i,j}(1 - y_{i,j}^l) + (1 - \lambda_{i,j})y_{i,j}^l\}. \quad (9)$$

- Updates for $\boldsymbol{\lambda}$: for $i = 1, \dots, N$ and $j = 1, \dots, C$,

$$\begin{aligned} \lambda_{i,j} &\propto \exp \left\{ \sum_{k=1}^K r_{i,k} \mathbb{E}_q[\log \tau_{k,j}] + \sum_{l \in L(i)} \{y_{i,j}^l \mathbb{E}_q[\log \Psi_j^l] + (1 - y_{i,j}^l) \mathbb{E}_q[\log(1 - \Psi_j^l)]\} \right\}, \\ 1 - \lambda_{i,j} &\propto \exp \left\{ \sum_{k=1}^K r_{i,k} \mathbb{E}_q[\log(1 - \tau_{k,j})] + \sum_{l \in L(i)} \{(1 - y_{i,j}^l) \mathbb{E}_q[\log \Psi_j^l] + y_{i,j}^l \mathbb{E}_q[\log(1 - \Psi_j^l)]\} \right\}. \end{aligned} \quad (10)$$

- Updates for \mathbf{e}, \mathbf{f} : for $k = 1, \dots, K$ and $j = 1, \dots, C$,

$$e_{k,j} = \alpha + \sum_{i=1}^N r_{i,k} \lambda_{i,j}, \quad f_{k,j} = \beta + \sum_{i=1}^N r_{i,k} (1 - \lambda_{i,j}). \quad (11)$$

- Updates for \mathbf{r} : for $i = 1, \dots, N$ and $k = 1, \dots, K$,

$$r_{i,k} \propto \exp \left\{ \mathbb{E}_q[\log \pi_k] + \sum_{j=1}^C \{\lambda_{i,j} \mathbb{E}_q[\log \tau_{k,j}] + (1 - \lambda_{i,j}) \mathbb{E}_q[\log(1 - \tau_{k,j})]\} \right\}. \quad (12)$$

- Updates for \mathbf{m} : for $k = 1, \dots, K$,

$$m_k = \gamma + \sum_{i=1}^N r_{i,k}. \quad (13)$$

For the beta distribution, the expectation of $\log \Psi_j^l$ and $\log(1 - \Psi_j^l)$ under q in (10) is:

$$\mathbb{E}_q[\log \Psi_j^l] = \psi(g_j^l) - \psi(g_j^l + h_j^l), \quad \mathbb{E}_q[\log(1 - \Psi_j^l)] = \psi(h_j^l) - \psi(g_j^l + h_j^l), \quad (14)$$

where $\psi(\cdot)$ is the digamma function. Similarly, we have $\mathbb{E}_q[\log \tau_{k,j}] = \psi(e_{k,j}) - \psi(e_{k,j} + f_{k,j})$, $\mathbb{E}_q[\log(1 - \tau_{k,j})] = \psi(f_{k,j}) - \psi(e_{k,j} + f_{k,j})$, and $\mathbb{E}_q[\log \pi_k] = \psi(m_k) - \psi(\sum_{i=1}^K m_k)$ in (12).

The per-iteration computational complexity of the algorithm is $\mathcal{O}(C(KN + LT))$, which scales linearly with C, K, N, L, T (T is the number of annotations that each annotator provides). Once the algorithm converges, our estimation of the ground truth $z_{i,j}$ is given by $\lambda_{i,j}$, which indicates the posterior probability of the instance i having the label j . Moreover, the reliability of annotators Ψ_j^l can be estimated by $g_j^l / (g_j^l + h_j^l)$ and the distribution P over 2^C distinct label combinations can be estimated by

$$\hat{P} = \left\{ p_S \mid p_S = \sum_{k=1}^K \mathbb{E}_q[\pi_k] \prod_{j \in S} \mathbb{E}_q[\tau_{k,j}] \prod_{j \in \{1,2,\dots,C\} \setminus S} (1 - \mathbb{E}_q[\tau_{k,j}]), S \subseteq \{1,2,\dots,C\} \right\}, \quad (15)$$

where $\mathbb{E}_q[\pi_k] = m_k$ and $\mathbb{E}_q[\tau_{k,j}] = \frac{e_{k,j}}{e_{k,j} + f_{k,j}}$. In the next section, we will show how well \hat{P} serves as an estimator of P (see Figure 5c for an illustration).

4 Experiments

We show that our proposed BMMB model outperforms the BNC model and several other competitive alternatives in terms of recovering ground truth labels. The experiments also reveal that the mixture of multiple independent Bernoulli distribution is able to accurately capture most of label interactions observed in the real dataset.

4.1 Datasets and Annotation Setup

Our experiments are based on three real-world multi-label datasets, as described in the follows:

- **Emotions**. The Emotions [23] dataset contains 593 pieces of music, each of which is associated with six possible pre-defined emotional tags, such as "happy-pleased" and "sadly-lonely".
- **Enron**. The Enron [25] is a dataset of emails. Each email is assigned with a subset of pre-defined categories based on genre, content, topic, or tone. There are 1,702 instances and 53 categories.
- **NUS-WIDE-SCENE**. The NUS-WIDE-SCENE [4] is a collection of images with real-world scenes, such as airport, ocean, and valley. It consists of 33 scene categories. We randomly sample 3,500 instances from the entire dataset.

To demonstrate the advantage of taking heterogeneous user reliability into account for annotation aggregation, as well as to verify how well our proposed models can recover their reliability, we generate noisy annotations of data samples from multiple annotators with varying quality. Following the setup in [20], we assume that there are three types of annotators: reliable, normal, and random. For reliable annotators, their reliability score Ψ_j^l is sampled from $\text{Uni}(0.85, 0.99)$. The reliability score of normal annotators is sampled from $\text{Uni}(0.66, 0.85)$. Finally, those random annotators have $\Psi_j^l = 0.5$. Moreover, we are interested in analyzing the behavior of different methods with respect to the sparsity of annotations. In particular, we allow each annotator to label varying number of instances. In the sequel, we use R to denote the ratio of three types of annotators (heterogeneity ratio) and T as the number of instances annotated by each user.

4.2 Experimental Settings

Hyperparameters. In both BNC and BMMB models, we choose the hyperparameters a and b based on the average number of annotations received by each instance. If the average number is less than two, we set $a = 12, b = 1$; otherwise, if it is less than four, we choose a weaker prior with $a = 6, b = 1$; in all other cases, $a = 4, b = 1$. We put a weak prior³ over τ with $\alpha = 0.06, \beta = 0.84$. Finally, for the BMMB model, we set $\gamma = 1/K$.

Termination Criterion. We run the inference algorithms until the relative improvement in the ELBO is less than a threshold $\eta = 0.0001$ or the program reaches the maximum number of iterations (MAXITER = 500).

Competing Algorithms. We compare our methods with the following algorithms:

- **Majority voting (MV).** If a label appears in more than half of annotations received by an instance, then we predict the instance to have that label. Although MV is easy to implement, it suffers from those random and adversarial annotators.
- **Power set+iBCC.** The iBCC model [15] is a Bayesian method to perform *multi-class* annotation aggregation. To apply the iBCC in the multi-label setting, a direct approach would be to treat each label combination as a class, resulting in 2^C distinct classes. We only run this algorithm when C is small due to the exponential number of label combinations.
- **Pairwise+iBCC.** It is a method that applies the iBCC to the subsets of label combinations formed from pairing labels [9]. The algorithm doesn't scale well either due to the exponential number of pairing schemes.

4.3 Results

Impact of annotator reliability. First, we vary the heterogeneity ratio R from 7:7:0 (no random annotators) to 4:4:6 (more than 40% are random annotators), and evaluate the performance of different algorithms in terms of recovering ground truth labels. As shown in Figure 3, BMMB outperforms all competing methods across all values of R , with BNC being the second best algorithm. Moreover, as expected, the performance gap between our proposed methods and majority voting tends to increase with the ratio of unreliable annotators. Finally, on the Emotions dataset where it is possible to run Powerset+iBCC and Pairwise+iBCC, the performance gap increases less significantly because iBCC also models the annotator reliability.

Impact of annotation sparsity. Next, we vary the number of instances annotated by each user from $T = 1$ to $T = 6$, and evaluate the behavior of the different algorithms with respect to annotation sparsity. The results are reported in Figure 4. Overall, the proposed models still have better performance across different levels of annotation sparsity, with the best performance achieved at the least sparsity level ($T = 6$). Again, the gap between BMMB and BNC demonstrates the effectiveness of modeling label dependency.

³The values of α, β don't have strong influence on the results as long as they are small enough.

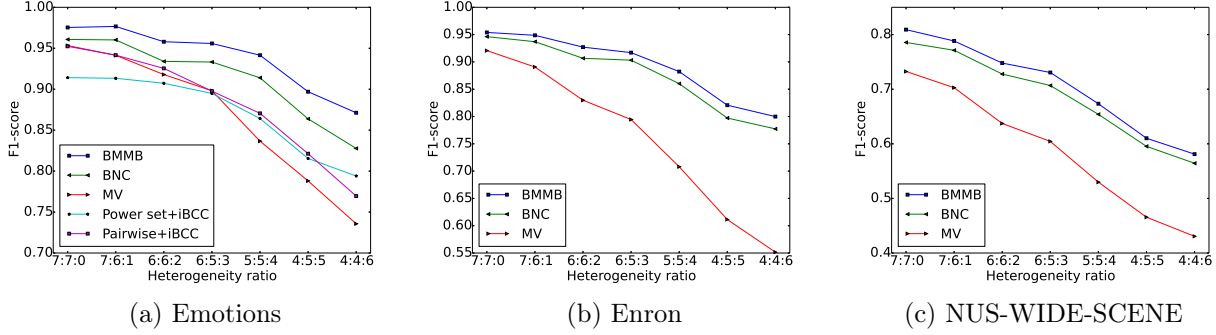


Figure 3: Impact of annotator reliability on recovering ground truth labels (evaluated by F1-score) of three datasets. The number of annotators L is 700, 2100, and 2100, respectively. The number of mixture components K is 6, 8, and 6, respectively. Each annotator provides $T = 5$ annotations.

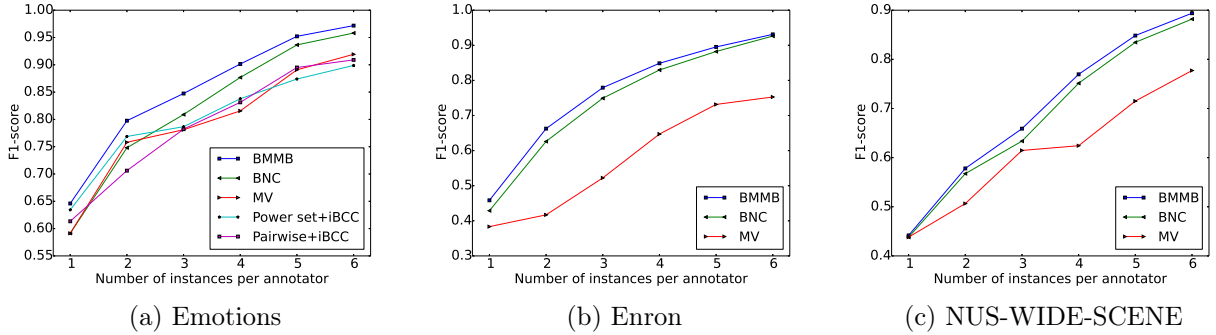


Figure 4: Impact of annotation sparsity on recovering ground truth labels (evaluated by F1-score) of three datasets. The number of annotators L is 900, 2700, and 4500, respectively. The number of mixture components K is 6, 8, and 6, respectively. The heterogeneity ratio of annotators $R = 1:1:1$.

Estimation of label dependency. All orders of label dependency can be captured if we have access to the ground truth probability $P = \{p_S \mid S \subseteq \{1, 2, \dots, C\}\}$ for each label combination. Given that $|P| = 2^C$, we can only use the Emotions dataset ($C = 6$) to demonstrate how well the BMMB estimator \hat{P} (15) can approximate the ground truth. Figure 5a and 5b present the KL divergence between P and \hat{P} with different values of K and L , and Figure 5c shows the element-wise difference between P and one \hat{P} estimated with $K = 6$ and $L = 900$. It is clear from Figure 5a that the performance gain from increasing K is quite marginal once K goes beyond 5. This is because not all label interactions are salient when the sample size is limited, as shown in Figure 5c. In this case, a fairly small number of mixture components is enough to capture most of label interactions observed in the dataset.

Estimation of annotator reliability. In this part, we evaluate the estimation of annotator reliability by examining if our proposed methods can successfully recover the type of annotators (reliable, normal, and random). To assign an annotator type for the user l , we average the estimated reliability score Ψ_j^l across all labels. As shown in Figure 6, the recovery rate of our methods rapidly increases with the number of annotated instances.

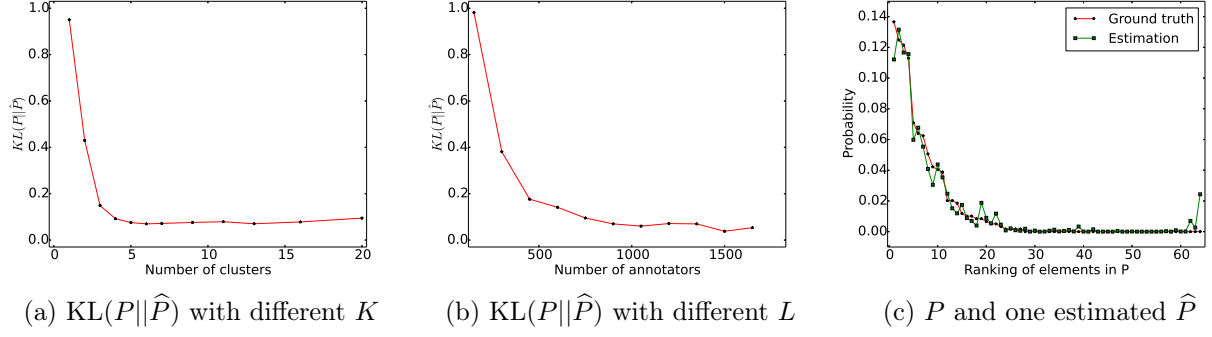


Figure 5: Estimation of label dependency on the Emotions dataset. The heterogeneity ratio of annotators $R=1:1:1$ and each annotator provides $T=5$ annotations. (a) We vary K from 1 to 20 with $L=900$. (b) We vary L from 150 to 1650 with $K=6$. (c) The element-wise difference between P and one \hat{P} estimated with $K=6$ and $L=900$. For clarity of presentation, we have sorted the elements of \hat{P} according to their ranking in P .

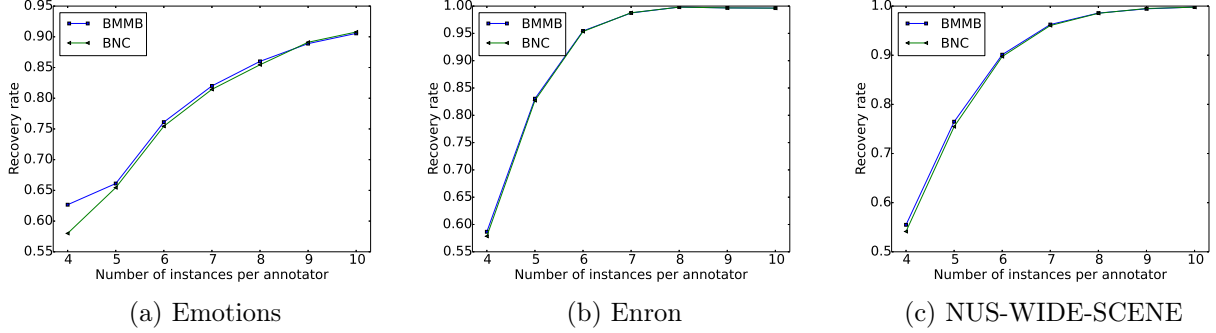


Figure 6: Recovery rate of the annotator type with $R=1:1:1$. The number of annotators L is 900, 2700, and 4500, respectively. For the BMMB model, K is 6, 8, and 6, respectively.

Impact of K . We have already demonstrated that a sufficiently large value of K would be enough to capture the label dependency. In this part, we show further evidence that the performance gain in terms of recovering ground truth labels (measured by F1-score) becomes marginal once K goes beyond some moderate value (Figure 7).

5 Conclusions and Implications

In this paper, we have shown how to exploit both annotator reliability and label dependency to perform multi-label annotation aggregation in a crowdsourcing scenario. Specifically, we propose flexible Bayesian models and efficient inference algorithms that make use of the mixture of multiple independent Bernoulli distribution. Experiments on real datasets confirm that our approaches outperform other competitive alternatives in terms of recovering ground truth labels. In addition, our method is able to recover the type of annotators with high accuracy, and the estimated model can well capture the observed label dependency. Encouraged by our results, in the future we plan to also

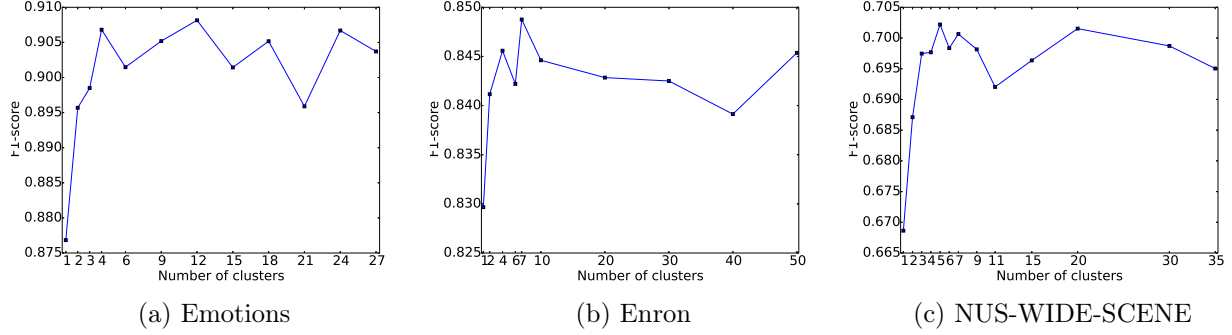


Figure 7: Impact of K on recovering ground truth labels (evaluated by F1-score) of three datasets with $R=1:1:1$ and $T=4$. The number of annotators L is 900, 2700, and 4500, respectively.

consider the clustering structure of annotators with similar behaviors [19] and use such information to further improve the performance.

Our research has several business implications. First, the proposed approach serves as a cost-effective tool to perform multi-label annotation aggregation. Although *multi-class* annotation aggregation has been well studied in the literature, the *multi-label* scenario still remains an important issue to be addressed. As demonstrated by the experimental results, our proposed model BMMB can improve the annotation accuracy by 10% – 30% (compared with majority voting) and 1% – 6% (compared with treating each label independently). This improvement will immediately translate into large differences in expense, given that certain big firms rely on such service on a daily basis [27] and that annotation collection is often the first step in the business process. Second, the crowdsourcing platforms can potentially utilize the estimated annotator reliability to build incentive mechanisms (e.g., performance-based payments [10]) so as to motivate workers to provide higher-quality annotations.

References

- [1] <https://crowdsource.google.com/imagelabeler/category>. 1
- [2] C. M. Bishop. *Pattern Recognition and Machine Learning*. Springer, 2006. 2
- [3] J. Bragg and D. S. Weld. Crowdsourcing multi-label classification for taxonomy creation. In *First AAAI conference on human computation and crowdsourcing*, 2013. 1
- [4] T.-S. Chua, J. Tang, R. Hong, H. Li, Z. Luo, and Y.-T. Zheng. NUS-WIDE: A real-world web image database from National University of Singapore. In *Proceedings of the ACM International Conference on Image and Video Retrieval*, 2009. 7
- [5] D. R. Cox. The analysis of multivariate binary data. *Applied Statistics*, 21(2):113–120, 1972. 2
- [6] B. Dai, S. Ding, and G. Wahba. Multivariate Bernoulli distribution. *Bernoulli*, 19(4):1465–1483, 2013. 2

- [7] A. P. Dawid and A. M. Skene. Maximum likelihood estimation of observer error-rates using the EM algorithm. *Journal of the Royal Statistical Society. Series C (Applied Statistics)*, 28(1):20–28, 1979. 2
- [8] A. Doan, R. Ramakrishnan, and A. Y. Halevy. Crowdsourcing systems on the world-wide web. *Communications of the ACM*, 54(4):86–96, 2011. 1
- [9] L. Duan, S. Oyama, H. Sato, and M. Kurihara. Separate or joint? Estimation of multiple labels from crowdsourced annotations. *Expert Systems with Applications*, 41(13):5723–5732, 2014. 4, 8
- [10] C.-J. Ho, A. Slivkins, S. Suri, and J. W. Vaughan. Incentivizing high quality crowdwork. In *Proceedings of the 24th International Conference on World Wide Web*, pages 419–429. ACM, 2015. 2, 11
- [11] P. G. Ipeirotis, F. Provost, and J. Wang. Quality management on amazon mechanical turk. In *Proceedings of the ACM SIGKDD workshop on human computation*, pages 64–67. ACM, 2010. 1
- [12] S. Jagabathula, L. Subramanian, and A. Venkataraman. Reputation-based worker filtering in crowdsourcing. In *Advances in Neural Information Processing Systems 27*, pages 2492–2500, 2014. 2
- [13] M. I. Jordan, Z. Ghahramani, T. S. Jaakkola, and L. K. Saul. An introduction to variational methods for graphical models. *Machine learning*, 37(2):183–233, 1999. 5
- [14] D. R. Karger, S. Oh, and D. Shah. Iterative learning for reliable crowdsourcing systems. In *Advances in neural information processing systems*, pages 1953–1961, 2011. 2
- [15] H.-C. Kim and Z. Ghahramani. Bayesian classifier combination. In *AISTAT*, pages 619–627, 2012. 2, 8
- [16] P. F. Lazarsfeld, N. W. Henry, and T. W. Anderson. *Latent Structure Analysis*. Houghton Mifflin, 1968. 2
- [17] C. Li, B. Wang, V. Pavlu, and J. Aslam. Conditional Bernoulli mixtures for multi-label classification. In *Proceedings of the 33rd International Conference on Machine Learning*, pages 2482–2491, 2016. 2
- [18] A. Moreno and C. Terwiesch. Doing business with strangers: Reputation in online service marketplaces. *Information Systems Research*, 25(4):865–886, 2014. 1
- [19] P. G. Moreno, A. Artes-Rodriguez, Y. W. Teh, and F. Perez-Cruz. Bayesian nonparametric crowdsourcing. *Journal of Machine Learning Research*, 16:1607–1627, 2015. 2, 11
- [20] D. Padmanabhan, S. Bhat, S. Shevade, and Y. Narahari. Topic model based multi-label classification. In *IEEE 28th International Conference on Tools with Artificial Intelligence*, pages 996–1003, 2016. 7
- [21] V. C. Raykar and S. Yu. Ranking annotators for crowdsourced labeling tasks. In *Advances in Neural Information Processing Systems 24*, pages 1809–1817. 2011. 2

- [22] V. C. Raykar, S. Yu, L. H. Zhao, G. H. Valadez, C. Florin, L. Bogoni, and L. Moy. Learning from crowds. *Journal of Machine Learning Research*, 11:1297–1322, 2010. [2](#), [3](#)
- [23] K. Trohidis, G. Tsoumakas, G. Kalliris, and I. P. Vlahavas. Multi-label classification of music into emotions. In *Proceedings of the 9th International Conference on Music Information Retrieval*, pages 325–330, 2008. [5](#), [7](#)
- [24] G. Tsoumakas and I. Katakis. Multi-label classification: An overview. *International Journal of Data Warehousing and Mining*, 3(3):1–13, 2007. [2](#)
- [25] G. Tsoumakas, E. Spyromitros-Xioufis, J. Vilcek, and I. Vlahavas. MULAN: A Java library for multi-label learning. *Journal of Machine Learning Research*, 12:2411–2414, 2011. [7](#)
- [26] M. J. Wainwright and M. I. Jordan. Graphical models, exponential families, and variational inference. *Foundations and Trends® in Machine Learning*, 1(1–2):1–305, 2008. [2](#), [5](#)
- [27] J. Wang, P. G. Ipeirotis, and F. Provost. Cost-effective quality assurance in crowd labeling. *Information Systems Research*, 28(1):137–158, 2017. [11](#)
- [28] J. Whitehill, T.-f. Wu, J. Bergsma, J. R. Movellan, and P. L. Ruvolo. Whose vote should count more: Optimal integration of labels from labelers of unknown expertise. In *Advances in neural information processing systems*, pages 2035–2043, 2009. [2](#)
- [29] M. Zhang and Z. Zhou. A review on multi-label learning algorithms. *IEEE Transactions on Knowledge and Data Engineering*, 26(8):1819–1837, 2014. [2](#), [4](#)
- [30] D. Zhou, S. Basu, Y. Mao, and J. C. Platt. Learning from the wisdom of crowds by minimax entropy. In *Advances in Neural Information Processing Systems*, pages 2195–2203, 2012. [2](#)

Appendix

A Details of Inference for the BMMB model

The exact form of the ELBO for the BMMB model is:

$$\begin{aligned}
\mathcal{L}(\theta_v) = & \sum_{l=1}^L \sum_{j=1}^C \sum_{i \in N(l)} \{ \lambda_{i,j} [y_{i,j}^l \mathbb{E}_q[\log \Psi_j^l] + (1 - y_{i,j}^l) \mathbb{E}_q[\log(1 - \Psi_j^l)]] \\
& + (1 - \lambda_{i,j}) [y_{i,j}^l \mathbb{E}_q[\log(1 - \Psi_j^l)] + (1 - y_{i,j}^l) \mathbb{E}_q[\log \Psi_j^l]] \} \\
& + \sum_{j=1}^C \sum_{l=1}^L \{ \log \Gamma(g_j^l + h_j^l) - \log \Gamma(g_j^l) - \log \Gamma(h_j^l) \} - LC[\log \Gamma(a + b) - \log \Gamma(a) - \log \Gamma(b)] \\
& + \sum_{j=1}^C \sum_{l=1}^L (a - g_j^l) \mathbb{E}_q[\log \Psi_j^l] + \sum_{j=1}^C \sum_{l=1}^L (b - h_j^l) \mathbb{E}_q[\log(1 - \Psi_j^l)] \\
& + \sum_{j=1}^C \sum_{k=1}^K \{ \log \Gamma(e_{k,j} + f_{k,j}) - \log \Gamma(e_{k,j}) - \log \Gamma(f_{k,j}) \} - KC[\log \Gamma(\alpha + \beta) - \log \Gamma(\alpha) - \log \Gamma(\beta)] \\
& + \sum_{j=1}^C \sum_{k=1}^K (\alpha - e_{k,j}) \mathbb{E}_q[\log \tau_{k,j}] + \sum_{j=1}^C \sum_{k=1}^K (\beta - f_{k,j}) \mathbb{E}_q[\log(1 - \tau_{k,j})] \\
& + \sum_{i=1}^N \sum_{k=1}^K r_{i,k} \sum_{j=1}^C \{ \lambda_{i,j} \mathbb{E}_q[\log \tau_{k,j}] + (1 - \lambda_{i,j}) \mathbb{E}_q[\log(1 - \tau_{k,j})] \} \\
& - \sum_{i=1}^N \sum_{j=1}^C \{ \lambda_{i,j} \log \lambda_{i,j} + (1 - \lambda_{i,j}) \log(1 - \lambda_{i,j}) \} + \sum_{i=1}^N \sum_{k=1}^K r_{i,k} \{ \mathbb{E}_q[\log \pi_k] - \log r_{i,k} \} \\
& + \log \Gamma(K\gamma) + \sum_{k=1}^K \log \Gamma(m_k) - K \log \Gamma(\gamma) - \log \Gamma\left(\sum_{k=1}^K m_k\right) + \sum_{k=1}^K (\gamma - m_k) \mathbb{E}_q[\log \pi_k].
\end{aligned} \tag{16}$$

B Details of Inference for the BNC model

The true posterior of latent variables $p(\Psi, \mathbf{z}, \tau | \mathbf{Y}, a, b, \alpha, \beta)$ is approximated by a fully factorized distribution $q(\Psi, \mathbf{z}, \tau)$ where

$$q(\Psi, \mathbf{z}, \tau) = q(\Psi | \mathbf{g}, \mathbf{h}) q(\mathbf{z} | \boldsymbol{\lambda}) q(\tau | \mathbf{e}, \mathbf{f}). \tag{17}$$

The ELBO for the BNC model is:

$$\begin{aligned}
\mathcal{L}(\theta_v) = & \sum_{l=1}^L \sum_{j=1}^C \sum_{i \in N(l)} \{ \lambda_{i,j} [y_{i,j}^l \mathbb{E}_q[\log \Psi_j^l] + (1 - y_{i,j}^l) \mathbb{E}_q[\log(1 - \Psi_j^l)]] \\
& + (1 - \lambda_{i,j}) [y_{i,j}^l \mathbb{E}_q[\log(1 - \Psi_j^l)] + (1 - y_{i,j}^l) \mathbb{E}_q[\log \Psi_j^l]] \} \\
& + \sum_{j=1}^C \sum_{l=1}^L \{ \log \Gamma(g_j^l + h_j^l) - \log \Gamma(g_j^l) - \log \Gamma(h_j^l) \} - LC [\log \Gamma(a + b) - \log \Gamma(a) - \log \Gamma(b)] \\
& + \sum_{j=1}^C \sum_{l=1}^L (a - g_j^l) \mathbb{E}_q[\log \Psi_j^l] + \sum_{j=1}^C \sum_{l=1}^L (b - h_j^l) \mathbb{E}_q[\log(1 - \Psi_j^l)] \\
& + \sum_{j=1}^C \{ \log \Gamma(e_j + f_j) - \log \Gamma(e_j) - \log \Gamma(f_j) \} - C [\log \Gamma(\alpha + \beta) - \log \Gamma(\alpha) - \log \Gamma(\beta)] \\
& + \sum_{j=1}^C (\alpha - e_j) \mathbb{E}_q[\log \tau_j] + \sum_{j=1}^C (\beta - f_j) \mathbb{E}_q[\log(1 - \tau_j)] \\
& + \sum_{i=1}^N \sum_{j=1}^C \{ \lambda_{i,j} \{ \mathbb{E}_q[\log \tau_j] - \log \lambda_{i,j} \} + (1 - \lambda_{i,j}) \{ \mathbb{E}_q[\log(1 - \tau_j)] - \log(1 - \lambda_{i,j}) \} \}.
\end{aligned} \tag{18}$$

The update rules are as follows:

- The update equations for \mathbf{g}, \mathbf{h} are the same as the ones (9) in the BMMB model.
- Updates for $\boldsymbol{\lambda}$: for $i = 1, \dots, N$ and $j = 1, \dots, C$,

$$\begin{aligned}
\lambda_{i,j} & \propto \exp \left\{ \mathbb{E}_q[\log \tau_j] + \sum_{l \in L(i)} \{ y_{i,j}^l \mathbb{E}_q[\log \Psi_j^l] + (1 - y_{i,j}^l) \mathbb{E}_q[\log(1 - \Psi_j^l)] \} \right\}, \\
1 - \lambda_{i,j} & \propto \exp \left\{ \mathbb{E}_q[\log(1 - \tau_j)] + \sum_{l \in L(i)} \{ (1 - y_{i,j}^l) \mathbb{E}_q[\log \Psi_j^l] + y_{i,j}^l \mathbb{E}_q[\log(1 - \Psi_j^l)] \} \right\}.
\end{aligned} \tag{19}$$

- Updates for \mathbf{e}, \mathbf{f} : for $j = 1, \dots, C$,

$$e_j = \alpha + \sum_{i=1}^N \lambda_{i,j}, \quad f_j = \beta + \sum_{i=1}^N (1 - \lambda_{i,j}). \tag{20}$$

Similar to the BMMB model, we have $\mathbb{E}_q[\log \Psi_j^l] = \psi(g_j^l) - \psi(g_j^l + h_j^l)$, $\mathbb{E}_q[\log(1 - \Psi_j^l)] = \psi(h_j^l) - \psi(g_j^l + h_j^l)$, $\mathbb{E}_q[\log \tau_j] = \psi(e_j) - \psi(e_j + f_j)$, and $\mathbb{E}_q[\log(1 - \tau_j)] = \psi(f_j) - \psi(e_j + f_j)$, where $\psi(\cdot)$ is the digamma function.